

Low energy cost high electro dialysis performance anion-exchange membranes for desalination

Shixi Zhong^{a,b}, Haonan Tie^{a,b}, Shijun Liao^{a,b,*}, Xiuhua Li^{a,b,*}

^aSchool of Chemistry and Chemical Engineering, South China University of Technology, Guangzhou 510641, China, Tel./Fax: +8620–22236591; emails: chsjliao@scut.edu.cn (S.J. Liao), lixiuhua@scut.edu.cn (X.H. Li), 787911341@qq.com (S.X. Zhong), 894225969@qq.com (H.N. Tie)

^bKey Laboratory of Fuel Cell Technology of Guangdong Province, South China University of Technology, Guangzhou 510641, China

Received 4 March 2019; Accepted 1 September 2019

ABSTRACT

Energy consumption (EC) and salt flux (J) are the two key parameters of the industrial electro dialysis (ED) devices. Increasing J usually increases EC. The challenge of a qualified ED anion-exchange membrane (AEM) is the dilemma of high J and low EC. Here we designed a series of poly(aromatic ethers) based AEMs with main-chain type quaternary ammoniums. The characterization results of structure and basic properties tell that the so-made AEMs are homogeneous, dense and defect-free, and show applicable ion exchange capacities (IECs), water uptakes (WUs), area resistances (R_{area}) and mechanical properties. The results of the ED tests clear that the current efficiency (η) values of the AEMs ED units are higher than 87.4% accompanying comparable or better EC than that of the commercial AEM TWEDA1 ED unit ($J = 81.22 \text{ mg m}^{-2} \text{ s}^{-1}$, $EC = 2.13 \text{ kWh kg}^{-1}$) and J varying from 79.77 to 80.92 $\text{mg m}^{-2} \text{ s}^{-1}$. Especially, the ED unit of QPAEK ($IEC = 1.14 \text{ mmol g}^{-1}$) has an EC of 2.08 kWh kg^{-1} . The tailored AEMs ED units have good comprehensive ED performances with relatively high J and low EC. These results reveal the potential of QPAEs for industrial ED processes.

Keywords: Anion exchange membrane; Poly(arylene ethers); Electro dialysis; Desalination; Low energy consumption

1. Introduction

The electro dialysis (ED) process is a method used to separate ionic species from non-ionic species in aqueous solutions under provided direct current (DC) electric fields [1–7]. In recent years, ED technology has been applied in various fields such as desalination of seawater, sea-salt production [8–11], food industry [12–14], industrial wastewater treatment [15–18] and so on. The advantages of ED over other separation processes include low energy consumption (EC), low cost of maintenance and fewer pre-treatment requirements [19].

As the key components of ED devices, ion exchange membranes (IEMs) have the ability to conduct counter-ions

and insulating co-ions resulting from the ionic groups fixed on the backbones, which has been called Donnan effect [20]. The selective transport of various ions of the IEMs is the base of ED [21]. IEMs have been divided into two kinds according to their fixed ionic groups, anion-exchange membrane (AEM) and cation exchange membrane (CEM). CEMs have been commercialized for many years due to the reliable and mature synthesis technique [22], while the properties and synthesis technique of ED AEMs are holding large spaces of improvements. To overcome the shortages of short lifetime undergoing high-density current and the high cost used in ED devices, various AEMs with different chemistry have been developed. The reported AEMs backbones include polyethylene [23,24], polystyrene [25,26], polyacrylate [27],

* Corresponding authors.

polyphenyl [28], poly(aromatic ether sulfones) [29–31], poly(phenylene oxides) [32,33], poly(aromatic ether ketones) (PAEKs) [34,35], polybenzimidazole [36], etc. While the fixed positive charged groups are rich in types of pyridinium [37], quaternary ammoniums [38], guanidinium [39], imidazolium [37,40], metal cationic groups [41], quaternary phosphonium [42]. To offer better ED performances, the specific AEMs with higher transport numbers (t) and lower area resistances (R_{area}) are necessary [43]. Chen's [44] work disclosed that an internal cross-linked bipyridinium AEM BPPO-20 ($t = 0.97$, $R_{\text{area}} = 2.45 \Omega \text{ cm}^2$) had better ED performances ($\eta = 95.2\%$, $\text{EC} = 5.97 \text{ kWh kg}^{-1}$, $J = 89.00 \text{ mg m}^{-2} \text{ s}^{-1}$) than that of a commercial membrane Neosepta AMX ($\eta = 94.1\%$, $\text{EC} = 6.51 \text{ kWh kg}^{-1}$, $J = 86.80 \text{ mg m}^{-2} \text{ s}^{-1}$) [44], where η is current efficiency, EC is energy consumption and J is salt flux. Khan et al. [19] fabricated a BPPO-based AEMs quaternized by dimethylethanolamine (DMEA) with t value high to 0.98 and R_{area} value low to $1.43 \Omega \text{ cm}^2$, DMEA-15, which offered η of 88.2%, J of $132.81 \text{ mg m}^{-2} \text{ s}^{-1}$ at EC high to $29.19 \text{ kWh kg}^{-1}$ [19]. Manohar et al. [45] work reported a PPO-based AEM with t the value of 0.98, AEM-3, gave out the ED test results of η and J of 83.4% and $21.33 \text{ mg m}^{-2} \text{ s}^{-1}$ respectively at EC of 6.53 kWh kg^{-1} . Chakrabarty et al. [46] work about a 2-(dimethylamino) ethylmethacrylate based ED AEM with t the value of 0.90, AEM-008, cleared that the values of η , EC and J were 78.5%, 4.77 kWh kg^{-1} and $42.67 \text{ mg m}^{-2} \text{ s}^{-1}$ individually [46]. Shah et al. [47] confirmed the importance of good membrane conductivity, IPA with R_{area} high of $5.32 \Omega \text{ cm}^2$ showed a very low J of $7.92 \text{ mg m}^{-2} \text{ s}^{-1}$ at η of 93.4% and EC of 0.49 kWh kg^{-1} [47]. Up to now, the challenge of qualified ED AEMs has been the dilemma of high J and low EC. The new synthesis technology for ED AEM should be developed to offer comprehensive performances with a good balance of production capacity and EC.

Our previous works have disclosed that the poly(aromatic ether sulfone) based main-chain ionic AEM QPAES-c overwhelms the other candidates with side-chain quaternary ammoniums and commercial ED AEM, TWEDA1, in the ED competition and shows an excellent desalination performance ($\eta = 0.949$, ED lifetime comparable to that of TWEDA1) [48]. Tuning the backbones of main-chain ionic AEMs is potentially helpful to yield good ED AEM candidates to solve above the above-mentioned challenge in ED processes. In this work, we synthesized three kinds of poly(arylene ethers) based main-chain ionic AEMs and systematically evaluate their ED performances in terms of η , J and EC. The structures of ionomers and their based AEMs were characterized by $^1\text{H-NMR}$, attenuated total reflection Fourier-transform infrared spectroscopy (ATR-FTIR) and scanning electron microscopy (SEM). To distinguish the so-made ED AEMs from the current ones, TWEDA1 was assessed under the same conditions. The ion exchange capacity (IEC), water uptake (WU), hydration number (λ), area resistance (R_{area}), mechanical properties and transport number (t) were also determined.

2. Experimental setup

2.1. Materials

4,4'-difluorodiphenyl ketone (FPK) and 4,4'-difluorodiphenyl sulfone (FPS) was purchased from Tokyo Chemical

Industry Co. Ltd., Tokyo, Japan. 1,1,2,2-tetrachloroethane (TCE), azodiisobutyronitrile (AIBN), N,N-Dimethylacetamide (DMAc), and N-bromosuccinimide (NBS) were purchased from Aladdin Reagent, Shanghai, China. 2,2',6,6'-tetramethyl biphenol (TMBP) was synthesized by the method reported before [49]. Three kinds of poly(aromatic ethers) (PAEs), PAEK ($m = 1$), poly(aromatic ether ketone sulfone) (PAEKs) ($m = 0.5$) and poly(aromatic ether sulfone) (PAES) ($m = 0$), were synthesized according to the previous work [50], where m is given out by Eq. (1).

$$m = \frac{n_{\text{FPK}}}{n_{\text{FPK}} + n_{\text{FPS}}} \quad (1)$$

where n_{FPK} and n_{FPS} are the feedings in a mole of FPK and FPS in the copolymerizations respectively. The gel permeation chromatography (GPC) analysis results of PAEs are as follows. PAEK: $M_n = 42 \text{ kg mol}^{-1}$, $M_w = 78 \text{ kg mol}^{-1}$, $M_w/M_n = 1.7$; PAEKs: $M_n = 47 \text{ kg mol}^{-1}$, $M_w = 83 \text{ kg mol}^{-1}$, $M_w/M_n = 1.7$; PAES: $M_n = 61 \text{ kg mol}^{-1}$, $M_w = 107 \text{ kg mol}^{-1}$, $M_w/M_n = 1.7$. The commercial AEM TWEDA1 was purchased from Shandong Tianwei Membrane Technology Co. Ltd., China. All the other solvents and reagents in the work were of analytical grade and used as received from the commercial chemical reagents companies.

2.2. Fabrications of quaternized poly(arylene ethers) Membranes

2.2.1. Synthesis of brominated poly(arylene ethers)

Brominated poly(arylene ethers) (BPAEs) were synthesized as shown in Fig. 1. A typical procedure of brominations of PAEs was as follows. A 100 mL round bottom three-necked flask installed the Dean-Stark manifold, a magnetic stirrer, and the N_2 inlet and outlet. PAEK (1.8263 g, 4 mmol) was introduced into the flask with 40 mL of TCE. After dissolving, AIBN (0.0657 g, 0.9 mmol) and NBS (1.0679 g, 6 mmol) were added. At the reaction temperature of 80°C for 4 h under nitrogen protection the reaction completed by cooling down to room temperature. The reaction mixture was dropped into 200 mL of methanol. The crude precipitated product was washed three times with methanol and dried under vacuum at 60°C for 24 h giving brominated PAEK (BPAEK). Brominated PAEKs and PAES (BPAEKs and BPAES) were obtained following a similar procedure.

2.2. Membranes preparation and quaternization

The following steps of the fabrications of quaternized membranes were depicted as Figs. 1(2–3). The casting solution of the brominated polymer BPAEK was fabricated by dissolving 1 g BPAEK in 7 mL of TCE. The solution was cast on a flat glass plate at room temperature for 48 h at least to let TCE volatile completely. Then, the membrane was peeled off and immersed in aqueous trimethylamine (TMA) (33 wt.%) for 48 h at room temperature to give quaternized PAEK membrane (QPAEK). The QPAEK membrane was washed by deionized water several times and kept in deionized water before analysis. The other quaternized BPAEs membranes (QPAEs), quaternized PAEKs and QPAES membranes (QPAEKs and QPAES) were obtained following the same procedure.

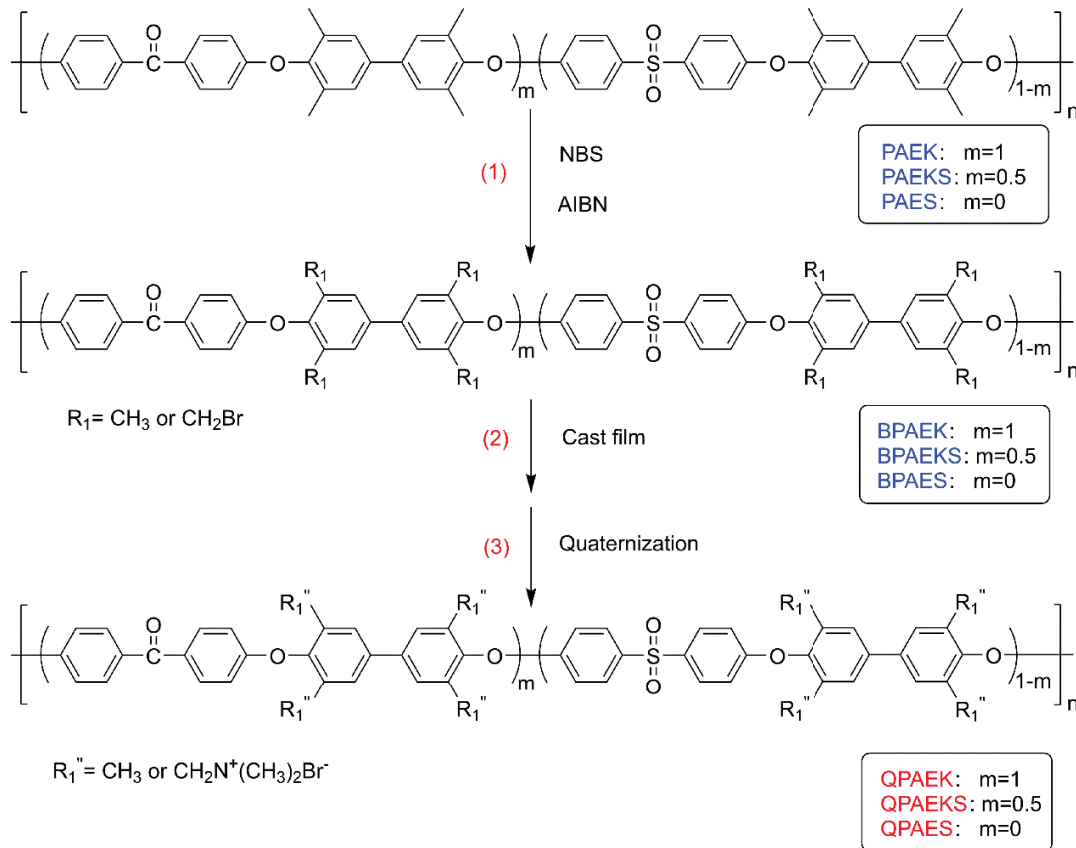


Fig. 1. Fabrications of quaternized poly(arylene ethers) membranes.

2.4. Characterization and measurements

2.4.1. $^1\text{H-NMR}$, ATR-FTIR and SEM

$^1\text{H-NMR}$ spectra were obtained on a Bruker Avance 400S (Bruker, Germany) with deuterated chloroform or dimethyl sulfoxide (CDCl_3 or DMSO-d_6), and tetramethylsilane (TMS) as the solvent and the standard respectively. ATR-FTIR spectra were obtained on a Bruker Vertex 70 instrument (Bruker, Germany). The surface and cross-section morphology images of the membranes were observed by a Hitachi S-3700N SEM instrument (Hitachi, Japan) with an accelerating voltage of 15 kV.

2.4.2. IEC, WU, hydration number (λ), area resistance (R_{area}) and mechanical properties

Back titrations were used to measure the IEC values of the quaternized poly(arylene ethers) membranes. Membrane samples cut into $3 \times 3 \text{ cm}^2$ size were immersed in 1 M NaOH at room temperature for 48 h to exchange Br^- with OH^- , then washed with deionized water to remove NaOH remaining on the surface. Each sample was immersed in 50 mL standardized HCl solution (0.01 M) for 24 h to make sure that OH^- ions in the membranes were reacted with HCl completely. Then the HCl mixture was titrated with a standardized NaOH solution (0.01 M) with phenolphthalein as an indicator. The IEC values were obtained using the following equation:

$$\text{IEC} = \frac{V_{\text{HCl}}C_{\text{HCl}} - V_{\text{NaOH}}C_{\text{NaOH}}}{m_{\text{dry}} + (V_{\text{HCl}}C_{\text{HCl}} - V_{\text{NaOH}}C_{\text{NaOH}})(M_{\text{Br}^-} - M_{\text{Cl}^-})} \quad (2)$$

where m_{dry} (g) is the weight of the dried sample, V_{HCl} (mL) and V_{NaOH} (mL) are the fixed volume of the HCl solution and the consumed volume of the NaOH titrating solution, C_{HCl} (M) and C_{NaOH} (M) are the concentrations of the HCl and NaOH solutions, M_{Br^-} (g mol^{-1}) is the molar mass of Br^- ions and M_{Cl^-} (g mol^{-1}) is that of Cl^- ions.

The WU of a sample of QPAEs was determined as follows. A membrane sample of $0.5 \times 5 \text{ cm}^2$ was immersed in NaCl solution (0.1 M) at room temperature for 24 h. Then the sample was taken out and the weight of the wet membrane (W_{wet}) was measured immediately as soon as the solution on the surface of the membrane was wiped off with tissue paper. W_{dry} is the weight of the dry membrane measured after the sample membrane was dried at 60°C for 24 h in vacuo. The WU values were calculated as follows:

$$\text{WU}(\%) = \frac{W_{\text{wet}} - W_{\text{dry}}}{W_{\text{dry}}} \times 100\% \quad (3)$$

Hydration number (λ) shows the average number of water molecules combined with each quaternary ammonium group. λ is calculated by the following equation:

$$\lambda = \frac{WU}{M_{\text{H}_2\text{O}}} \times \frac{1,000}{\text{IEC}} \quad (4)$$

where $M_{\text{H}_2\text{O}}$ (g mol⁻¹) is the molar mass of water.

Area resistances (R_{area}) of QPAEs were measured by an IviumStat frequency response analyzer (Ivium, Netherlands) as the method mentioned in published works [51,52]. It used a two-electrode, alternating-current impedance method. The frequency ranging and oscillating voltage was set from 1 kHz to 1 MHz and 10 mV respectively. Before the tests, all the samples would be immersed into a 0.1 M NaCl solution for 24 h. The tests were conducted in the environment of 25°C, 0.1 M NaCl solution. R_{area} was given by the following equation:

$$R_{\text{area}} = RA \quad (5)$$

where A (cm²) is the area of the test sample. R (Ω) is the resistance of the sample membrane.

An Instron M3300 was used to measure the mechanical properties of the membrane samples (50 × 5 mm²). test speed of 5 mm min⁻¹ at 25°C and 100% RH.

2.4.3. Transport number

The anion transport numbers (t^-) of the QPAEs membranes were tested according to the reported method [53]. A two-compartment cell was cycled with 0.1 M (C_1) and 0.2 M (C_2) KCl solutions respectively, which was separated by the investigated membrane. Two calomel reference electrodes were set on both sides of the membrane closely. The potential (E_m) between the two sides of the membrane was recorded with an Avometer. The relationship between t^- and E_m was given by the following equation:

$$E_m = (2t^- - 1) \frac{RT}{F} \ln \frac{C_1}{C_2} \quad (6)$$

where R and F are gas constant (8.314 J mol⁻¹ K⁻¹) and faraday constant (96485 C mol⁻¹) respectively, T is the testing temperature (K).

2.4.4. ED tests

ED tests ran in a four-compartment home-made ED device. The device was separated into four compartments by a pair of Nafion-115[®] CEM and one piece of AEM to be evaluated. The effective areas of the membranes in the device were of 9 cm². The two middle compartments acted as diluting and a concentrating compartment respectively. Two NaCl solutions with equal concentration and volume of 0.1 M and 150 mL were pumped cyclically into the two middle compartments at the same flow rates of 10 mL min⁻¹ individually. Two side compartments equipped with ruthenium coated titanium cathode and anode were pumped cyclically with a Na₂SO₄ solution (0.2 M, 150 mL) at a flow rate of 10 mL min⁻¹. Two side compartments were isolated from the two middle compartments by CEM, which prevented the producing of Cl₂. The powers for the solutions circulations were provided by two peristaltic pumps. The DCs used in the tests were provided by a DC power supplier (KORAD KA3005D, China) at

the current density set constantly at 15 mA cm⁻². Before the tests, each compartment of the ED device was circulated with the corresponding solution for 20 min to remove air bubbles without the applied current. The ED tests were performed for 150 min, and the conductivities of the NaCl solutions in the diluted compartment were tested by a conductivity meter (Lei-ci DDS-307, China) when the tests finished. The changes in the conductivities of NaCl solutions tell out the changes in the concentrations of the NaCl solutions owing to the inherent relationship.

2.4.5. Efficiency assessment

The current efficiency (η), EC and J are important parameters for evaluating the performances of the ED process.

η was calculated by the following equation:

$$\eta = \frac{Z(C_0 - C_t)VF}{NIt} \times 100\% \quad (7)$$

where Z is the absolute valence of Cl⁻, V is the volume of the NaCl solution in the diluting compartment, F is Faraday constant (96485 C mol⁻¹), C_0 and C_t are the concentrations of the NaCl solution at time 0 and t during ED process, N is the number of repeating units ($N = 1$), I is the applied current ($I = 0.135$ A).

The EC was calculated by Eq. (8).

$$\text{EC} = \int_0^t \frac{uI}{(C_0 - C_t)VM_{\text{NaCl}}} dt \quad (8)$$

where u is the voltage of the ED device, M_{NaCl} is the molecular weight of NaCl.

J was calculated by the following equation:

$$J = \frac{(C_0 - C_t)V}{At} \quad (9)$$

3. Results and discussion

3.1. Synthesis and characterizations of BPAEs and QPAEs

The fabrications of BPAEs and QPAEs are shown in Fig. 1. The ¹H-NMR spectra of the detailed BPAEs polymers, BPAEK, BPAEKS and BPAES are displayed in Figs. 2a–c respectively. The peaks appearing from 2.1 to 2.2 ppm are contributed by benzylmethyl groups, while those signals locating at 4.4 ppm are donated by –CH₂Br groups. Which confirm the successful brominations of PAEs polymers. It is worth noting that two different kinds of benzylmethyl groups of BPAEK offer two signals of “a” and “a’” in Fig. 2b, which gives an integral ratio of about 1:1 resulting from the feeding ratio of FPK and FPS of 1:1 during the synthesis of PAEKS. The similar splitting of the benzylbromide groups appears as separated signals of “b” and “b’”. Whilst BPAEK and BPAES offer mono-peak signals for benzylmethyl and benzylbromide groups (Figs. 2a and c).

Fig. 3 shows the ATR-FTIR spectra of QPAEK, QPEKS, QPAES, and the commercial TWEDA1. The strong wide signals ranging from 3,700 to 3,000 cm⁻¹ are due to the strong

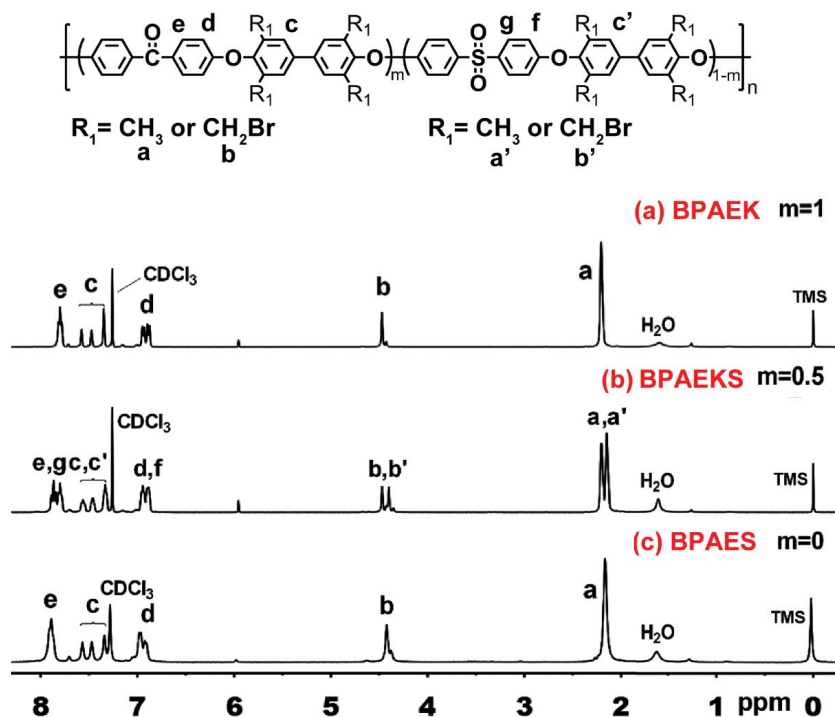


Fig. 2. $^1\text{H-NMR}$ spectra of (a) BPAEK, (b) BPAEKS, and (c) BPAES.

hydrophilicity of the quaternary ammonium bromides of QPAEs. The absorption bands at $2,922\text{ cm}^{-1}$ result from the stretching vibrations of C–H bonds of methyl groups. The strong bands at $1,640\text{ cm}^{-1}$ are attributed to the bending vibrations of H_2O . The characteristic absorptions of the C=C skeletal vibrations of aromatic rings are at $1,596$ and $1,498\text{ cm}^{-1}$. The stretching bands of Ar–O–Ar bonds occur at $1,108\text{ cm}^{-1}$. The bands at $1,185$ and $1,160\text{ cm}^{-1}$ are the stretching vibrations of C–N $^+$. The scissoring and wagging bands of methylene groups connecting with N $^+$ (Ar–CH $_2$ –N $^+$ (CH $_3$) $_3$) are at $1,468$ and $1,220\text{ cm}^{-1}$ respectively. These results confirm the success of quaternization. It is worth mentioning that bands at $1,293$ and $1,145\text{ cm}^{-1}$ in curves b and c are attributed by the stretching vibrations of O=S=O bonds and the absence of the absorption bands in curve a because of the monomers of QPAEK without FPS (Figs. 3a–c). Fig. 3d confirms the aliphatic skeleton of the commercial membrane TWEDA1.

3.2. Morphology of QPAEs

The SEM images of QPAEs are shown in Figs. 4a–f. The SEM surface and cross-section (fractured in liquid nitrogen) images of QPAEK, QPAEKS and QPAES show homogeneous and dense nature without any holes, cracks and phase separation at the magnifications of 6,000. The thicknesses of QPAEs membranes ranged from 110 to 130 μm , which are given by an Exploit dial-type thickness gauge.

3.3. IEC, WU, λ , R_{area} and mechanical properties of QPAEs

The IECs and WUs of QPAEs are shown in Fig. 5. The λ and R_{area} are depicted in Fig. 6. IEC has an important

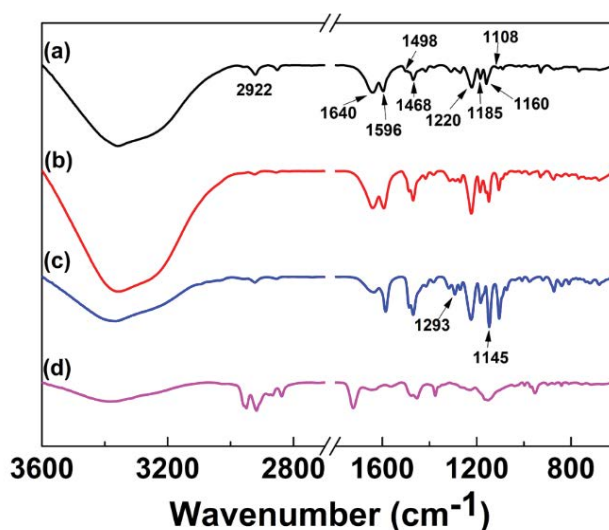


Fig. 3. ATR-FTIR spectra of QPAEs and TWEDA1: (a) QPAEK, (b) QPAEKS, (c) QPAES, and (d) TWEDA1.

impact on the performance of AEMs. Generally, membranes with high IECs have lower R_{area} and higher WU values. The three tailored membranes in this study have close IEC values ranging from 1.07 to 1.26 mmol g^{-1} . According to the Donnan equilibrium theory, the permeability and permselectivity of AEMs depend on the concentration of the fixed cationic group in the wet membranes. The higher the concentrations of the fixed groups the stronger the resulting electric fields, which provide stronger repulsion to the

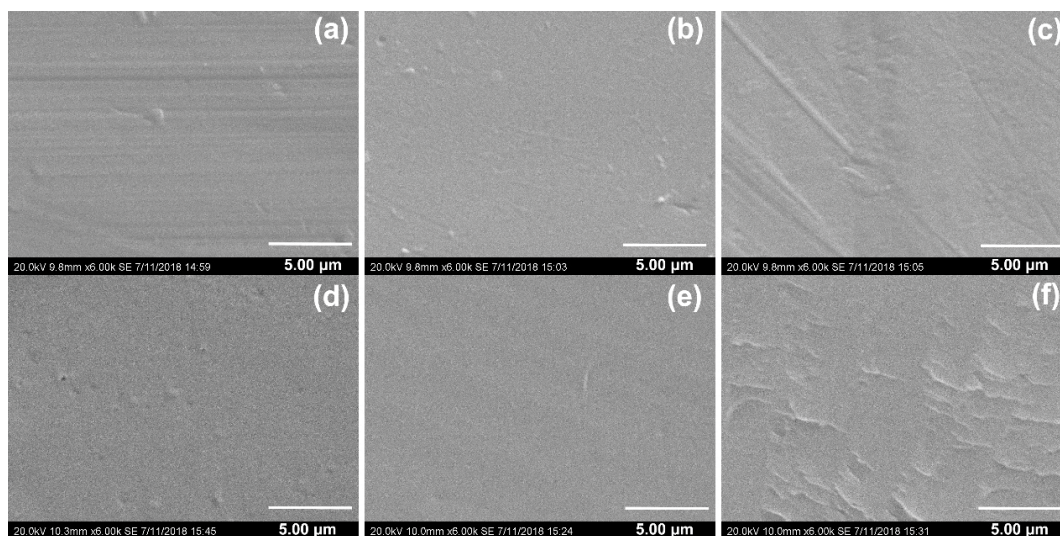


Fig. 4. SEM surface and cross-section images of QPAEs: (a) QPAEK (surface), (b) QPAEKS (surface), (c) QPAES (surface), (d) QPAEK (section), (e) QPAEKS (section), and (f) QPAES (section).

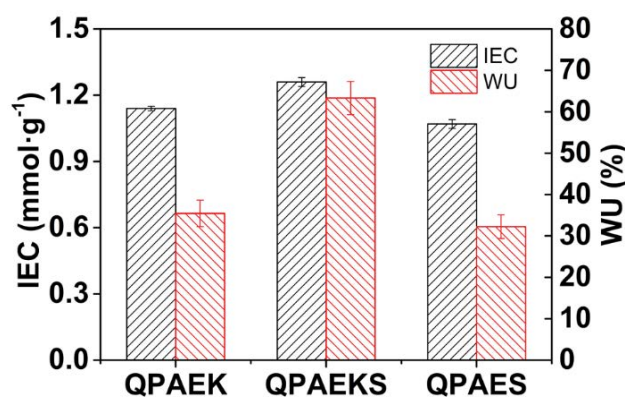


Fig. 5. IEC and WU of QPAEs at room temperature.

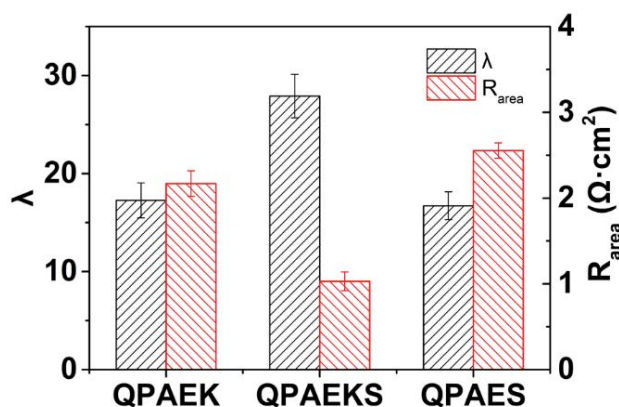


Fig. 6. λ and σ of QPAEs at room temperature.

co-ions. Within a certain range, increasing the IEC values of the dry AEMs can increase the concentration of the fixed cationic groups of the wet AEMs. However, over high IECs result in excessive WUs and decrease fixed groups concentrations of the wet AEMs. Moreover, excessive water absorption leads to a looser membranes structure, which weakens the molecular sieving effect causing decreases in permeability and permselectivity reflected by the decrease of transport number (t) [55]. Therefore, the IEC values of AEMs should be controlled to an appropriate range. The water absorption abilities of QPAEs change dramatically leading to WUs jump from 32.24 to 63.32 even the IEC window of QPAEs is narrow as 0.19 mmol g⁻¹. λ shows a similar tendency, which increases from 16.7 to 27.9. QPAEKS has about two times λ of that for QPAEK and QPAES. The highest λ offers the lowest local charge density in the group and changes the permeability and permselectivity of QPAEKS greatly. QPAEKS shows the highest ion conductivity with the lowest R_{area} of 1.03 $\Omega \text{ cm}^2$ and the poorest permselectivity with the lowest transport number value of 0.87 (Table 2).

The mechanical properties of QPAEs under the fully hydrated conditions at room temperature are listed in Table 1. The QPAEs membranes have tensile strengths of 13.9–18.5 MPa and elongations at break of 6.5%–66.2%. The tensile properties of QPAEs are comparable to that of the reported IEMs [40,54] and Nafion-117® [55]. All the QPAEs have run several times of ED tests and survived from the fixations of the ED equipment and the testing. This suggests that the mechanical properties of the QPAEs membranes are acceptable to satisfy the ED requirements.

3.4. Transport number

Transport number (t) is the fraction of the total electrical current carried in an AEM by the exchangeable anions. It is one of the most important parameters of ED AEMs, which clears the anion selectivity of the AEMs. The value of t of an ED AEM reflects the permselectivity level of the membrane without an extra DC field. Generally, AEMs with higher t values have better isolation abilities to cations. In this study,

Table 1
IEC values and mechanical properties of QPAEs and some of the reported IEMs

Membrane	IEC _{Theo} ^a /mmol g ⁻¹	IEC _{exp} ^b /mmol g ⁻¹	Tensile strength/MPa	Elongation at break/%
QPAEK	2.34	1.14 ± 0.01	18.5 ± 1.2	66.2 ± 2.4
QPAEKS	2.87	1.26 ± 0.02	16.1 ± 1.4	25.8 ± 2.1
QPAES	2.29	1.07 ± 0.02	13.9 ± 0.8	6.5 ± 1.0
M-1 [40]	–	1.14	28.9	7.2
PQSV-4 [54]	–	1.36	11.87	79.89
Nafion-117 [®] [55]	–	0.91	21.1	370.6

^aIEC_{theo} is calculated from bromination degree that supposing all re-active –Br have been replaced.

^bIEC_{exp} is calculated by the titration result.

Table 2
 η , EC and J of QPAEs and some reported ED AEMs

Membrane	IEC/mmol g ⁻¹	t^-	R_{area}/Ω cm ²	η /%	EC/kWh kg ⁻¹	J /mg m ⁻² s ⁻¹
QPAEK	1.14 ± 0.01	0.94	2.17 ± 0.15	88.2 ± 0.1	2.08 ± 0.03	80.52 ± 2.30
QPAEKS	1.26 ± 0.02	0.87	1.03 ± 0.11	87.4 ± 0.2	2.14 ± 0.03	79.77 ± 1.11
QPAES	1.07 ± 0.02	0.96	2.55 ± 0.09	88.7 ± 0.3	2.15 ± 0.04	80.92 ± 0.02
TWEDA1	1.01	0.94	–	89.0 ± 0.2	2.13 ± 0.02	81.22 ± 0.92
AEM-3 [45]	1.61	0.98	–	83.4	6.53	21.33
AEM-008 [46]	2.92	0.90	–	78.5	4.77	42.67
IPA [47]	1.69	0.92	5.32	93.4	0.49	7.92
BPPO-20 [44]	1.98	0.97	2.45	95.2	5.97	89.00
DMEA-15 [19]	1.47	0.98	1.43	88.2	29.19	132.81
MDPP-43 [56]	1.52	0.95	2.9	59.4	29.52	102.7

KCl solutions (0.1 M and 0.2 M) is used to calculate t^- by Eq. (5) instead of the NaCl solutions in the published works [2,53]. The reasons are that K⁺ and Cl⁻ have similar values of ion mobility in the diluted solution and the used method can eliminate the deviations resulted from the difference in ions mobility of Na⁺ and Cl⁻ during the measurements. Fig. 7 gives out t^- values of QPAEK, QPAEKS, and QPAES of 0.94, 0.87 and 0.96 respectively. The values of t^- decrease with rises in IECs and λ for the above-mentioned reasons and QPAES shows a better permselectivity than TWEDA1, which has t^- of 0.94.

3.5. ED performances

Current efficiency (η), EC and J are the basic parameters to assess the ED performance of the related key materials. η is defined as the ratio of experimental migration to the theoretical migration of Na⁺Cl⁻. EC is the EC per 1 kg NaCl migrating in ED device. J is the mass transport per membrane area and per time unit. Enough high J value of ED device tells out the industrial applied potential. A good ED AEM candidate should have the ability to balance the improvements in η and J and the increase in EC.

ED tests were performed in a homemade ED device, the η , EC and J data of each AEM sample were evaluated after a 150 min ED process under a constant current condition of 0.135 A. The concentration of NaCl solutions (C_1 and C_2) were obtained from the conductivity of the solutions, while η and EC were calculated according to Eqs. (6) and (7). These

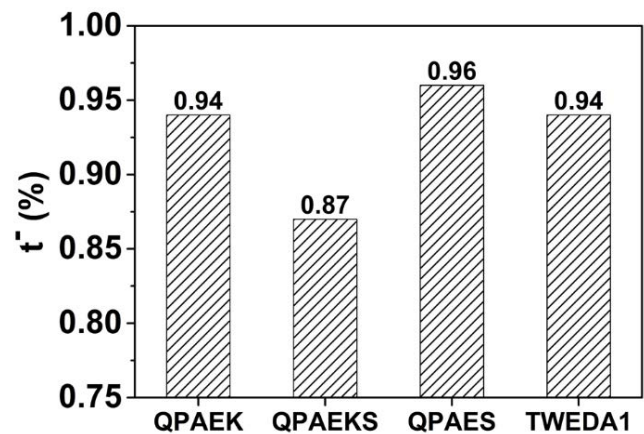


Fig. 7. t^- of QPAEs at room temperature.

results are shown in Fig. 8. To benchmark, the ED performances of QPAEs, the commercial ED AEM, TWEDA1, has run the same test and the corresponding data are displayed in Fig. 8 too. η can precisely reflect the permselectivity of AEMs under the conditions of the same ED device equipped with the same quality CEM. The higher the η value, the less the Na⁺ leakage of the AEM has under the DC fields. The η values of QPAEK, QPAEKS, QPAES in this work (88.2%, 87.4%, 88.7% respectively) are very close to that of TWEDA1 equaling 89.0%. EC under a constant current

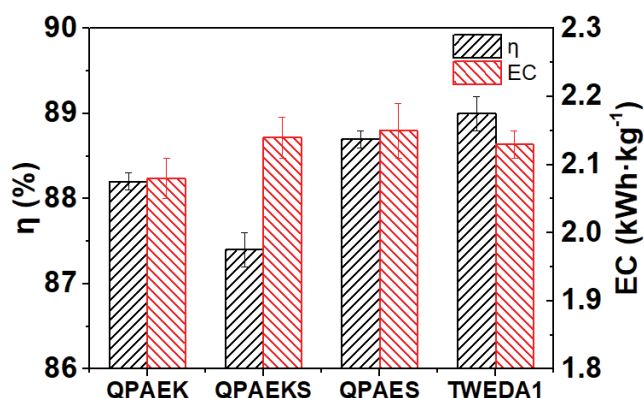


Fig. 8. η and ECs of the QPAEs and TWEDA1.

condition is controlled by three factors: permselectivities and resistances of IEMs, the deviations of the applied constant current from the varying limit currents of the dilute cell with the prolonging ED time. AEMs with lower IECs usually have better permselectivities playing a positive role in decreasing EC since the CEM has been fixed. However, lower IEC often results in lower ion conductivity or high electric resistance at the same membrane thickness and operation conditions. Since QPAEK, QPAEKs and QPAES have similar values of a thickness (130, 110, and 130 μm respectively), so the ion conductivities through the AEMs are controlled by the resistance of the used AEMs. Better conductivity of QPAEKs offsets the negative effect of the low t . The ECs of the ED units based on QPAEK, QPAEKs, and QPAES is 2.08, 2.14 and 2.15 kWh kg^{-1} individually. All the ED units based on the designed AEMs show similar EC values to that of the ED unit based on TWEDA1, which has an EC value of 2.13 kWh kg^{-1} . J values of the QPAEs ED units are very close to that of the TWEDA1 ED unit (81.22 $\text{mg m}^{-2} \text{s}^{-1}$) (Table 2), which has been calculated according to Eq. (8). Table 2 lists out the data of η , EC and J of some of the best candidates of the reported ED AEMs simultaneously. QPAEKs ED unit shows the lowest η value because of its highest IEC and WU. These features lead to its low J value. QPAEK ED unit shows the lowest EC and the comparable η and J to that of the TWEDA1 ED unit. Industrial ED devices prefer big J to ensure the productive capacity at the cost of partially increased EC. An excellent ED unit should balance the EC and J to satisfy the requirements of the industrial ED processes. The ED units based on BPPO-20 [44], DMEA-15 [19] and MDPP-43 [56] offer higher J values than that of the QPAEK ED unit with jumps less than 64.9%. However, their EC is 2.87–14.19 times of that of QPAEK ED unit. It should be noted that IPA ED units [47] give an extremely low EC value of 0.49 kWh kg^{-1} at J of 7.92 $\text{mg m}^{-2} \text{s}^{-1}$, which is about 10% of that of the ED units in this work. Moreover, the QPAEs ED units show much lower EC value at J times of those of the reported AEM-3 [45] and AEM-008 [46] ED units.

4. Conclusion

A series of designed PAEs based main chain ionic AEMs, QPAEK, QPAEKs and QPAES, were derived by successful brominations and quaternization of the mother polymers

from 4,4'-difluorodiphenyl sulfone, 4,4'-difluorodiphenyl ketone and 2,2',6,6'-tetramethyl biphenol. All the AEMs are homogeneous and dense in nature without any holes and cracks and show applicable IEC, WU, R_{area} and mechanical properties. The results of the ED tests clear that the η values of the ED units based on the tailored AEMs are higher than 87.4% accompanying comparable or better EC than that of the ED unit with the commercial AEM TWEDA1 ($J = 81.22 \text{ mg m}^{-2} \text{ s}^{-1}$; $\text{EC} = 2.13 \text{ kWh kg}^{-1}$). Especially, the ED unit of QPAEK ($\text{IEC} = 1.14 \text{ mmol g}^{-1}$; $\text{WU} = 35.46 \%$, $R_{\text{area}} = 2.17 \Omega \text{ cm}^2$) with the second-highest t of 0.94 has the lowest EC of 2.08 kWh kg^{-1} with a J of 80.52 $\text{mg m}^{-2} \text{ s}^{-1}$. It should be attributed to the balance between high permselectivity and moderate resistance. The tailored QPAEs AEMs ED units have good comprehensive ED performances with relatively high J and low EC. These results reveal the potential application of QPAEs for industrial ED processes.

Acknowledgments

This work was supported by the National Key R&D Program of China (No. 2017YFB0102900), Guangzhou Science Technology and Innovation Commission (No. 201804010436), the Research Fund of the Key Laboratory of Low Carbon Chemistry & Energy Conservation of Guangdong Province (No. 20170103), and the SRP Fund of South China University of Technology (Grant 105612018S177).

References

- [1] C. Klaysom, R. Marschall, L.Z. Wang, B.P. Ladewig, G.Q.M. Lu, Synthesis of composite ion-exchange membranes and their electrochemical properties for desalination applications, *J. Mater. Chem.*, 20 (2010) 4669–4674.
- [2] C. Klaysom, R. Marschall, S.-H. Moon, B.P. Ladewig, G.Q.M. Lu, L.Z. Wang, Preparation of porous composite ion-exchange membranes for desalination application, *J. Mater. Chem.*, 21 (2011) 7401–7409.
- [3] N. Tanaka, M. Nagase, M. Higa, Preparation of aliphatic-hydrocarbon-based anion-exchange membranes and their anti-organic-fouling properties, *J. Membr. Sci.*, 384 (2011) 27–36.
- [4] S. Mulyati, R. Takagi, A. Fujii, Y. Ohmukai, T. Maruyama, H. Matsuyama, Improvement of the antifouling potential of an ion exchange membrane by surface modification with a polyelectrolyte for an electro dialysis process, *J. Membr. Sci.*, 417 (2012) 137–143.
- [5] K.M. Majewska-Nowak, Treatment of organic dye solutions by electro dialysis, *Adv. Civ. Environ. Mater. Res.*, 4 (2013) 203–214.
- [6] S. Caprarescu, M.C. Corobea, V. Purcar, C.I. Spataru, R. Ianchis, G. Vasilevici, Z. Vuluga, San copolymer membranes with ion exchangers for Cu(II) removal from synthetic wastewater by electro dialysis, *J. Environ. Sci.-China*, 35 (2015) 27–37.
- [7] D.J. Wan, S.H. Xiao, X.Y. Cui, Q.H. Zhang, Y.H. Song, Removal of Cu^{2+} from aqueous solution using proton exchange membrane by Donnan dialysis process, *Environ. Earth Sci.*, 73 (2015) 4923–4929.
- [8] H. Strathmann, Electro dialysis, a mature technology with a multitude of new applications, *Desalination*, 264 (2010) 268–288.
- [9] K. Venugopal, S. Dharmalingam, Evaluation of synthetic salt water desalination by using a functionalized polysulfone based bipolar membrane electro dialysis cell, *Desalination*, 344 (2014) 189–197.
- [10] F.B. Luo, Y.M. Wang, C.X. Jiang, B. Wu, H.Y. Feng, T.W. Xu, A power free electro dialysis (PFED) for desalination, *Desalination*, 404 (2017) 138–146.
- [11] N.C. Wright, S.R. Shah, S.E. Amrose, A.G. Winter V., A robust model of brackish water electro dialysis desalination with

- experimental comparison at different size scales, *Desalination*, 443 (2018) 27–43.
- [12] F. Goncalves, C. Fernandes, P.C. dos Santos, M.N. de Pinho, Wine tartaric stabilization by electrodialysis and its assessment by the saturation temperature, *J. Food Eng.*, 59 (2003) 229–235.
- [13] E. Vera, J. Ruales, M. Dornier, J. Sandeaux, R. Sandeaux, G. Pourcelly, Deacidification of clarified passion fruit juice using different configurations of electrodialysis, *J. Chem. Technol. Biotechnol.*, 78 (2003) 918–925.
- [14] G.Q. Chen, F.I.I. Eschbach, M. Weeks, S.L. Gras, S.E. Kentish, Removal of lactic acid from acid whey using electrodialysis, *Sep. Purif. Technol.*, 158 (2016) 230–237.
- [15] F.L. Fu, Q. Wang, Removal of heavy metal ions from wastewaters: a review, *J. Environ. Manage.*, 92 (2011) 407–418.
- [16] F.D. Belkada, O. Kitous, N. Drouiche, S. Aoudj, O. Bouchelaghem, N. Abdi, H. Grib, N. Mameri, Electrodialysis for fluoride and nitrate removal from synthesized photovoltaic industry wastewater, *Sep. Purif. Technol.*, 204 (2018) 108–115.
- [17] X.-R. Pan, W.-W. Li, L. Huang, H.-Q. Liu, Y.-K. Wang, Y.-K. Geng, P.K.-S. Lam, H.-Q. Yu, Recovery of high-concentration volatile fatty acids from wastewater using an acidogenesis-electrodialysis integrated system, *Bioresour. Technol.*, 260 (2018) 61–67.
- [18] H. Selvaraj, P. Aravind, M. Sundaram, Four compartment mono selective electrodialysis for separation of sodium formate from industry wastewater, *Chem. Eng. J.*, 333 (2018) 162–169.
- [19] M.I. Khan, C.L. Zheng, A.N. Mondal, Md.M. Hossain, B. Wu, K. Emmanuel, L. Wu, T.W. Xu, Preparation of anion exchange membranes from BPPO and dimethylethanolamine for electrodialysis, *Desalination*, 402 (2017) 10–18.
- [20] F.G. Donnan, The theory of membrane equilibria, *Chem. Rev.*, 1 (1924) 73–90.
- [21] Y. Tanaka, A computer simulation of continuous ion exchange membrane electrodialysis for desalination of saline water, *Desalination*, 249 (2009) 809–821.
- [22] B.M. Asquith, J. Meier-Haack, C. Vogel, W. Butwilowski, B.P. Ladewig, Side-chain sulfonated copolymer cation exchange membranes for electro-driven desalination applications, *Desalination*, 324 (2013) 93–98.
- [23] M. Zhang, H.K. Kim, E. Chalkova, F. Mark, S.N. Lvov, T.C.M. Chung, New polyethylene based anion exchange membranes (PE-AEMs) with high ionic conductivity, *Macromolecules*, 44 (2011) 5937–5946.
- [24] N.J. Robertson, H.A. Kostalik, T.J. Clark, P.F. Mutolo, H.D. Abruna, G.W. Coates, Tunable high performance cross-linked alkaline anion exchange membranes for fuel cell applications, *J. Am. Chem. Soc.*, 132 (2010) 3400–3404.
- [25] C.R. Yang, S.L. Wang, W.J. Ma, L.H. Jiang, G.Q. Sun, Highly alkaline stable N1-alkyl substituted 2-methylimidazolium functionalized alkaline anion exchange membranes, *J. Mater. Chem. A*, 3 (2015) 8559–8565.
- [26] T.H. Tsai, A.M. Maes, M.A. Vandiver, C. Versek, S. Seifert, M. Tuominen, M.W. Liberatore, A.M. Herring, E.B. Coughlin, Synthesis and structure-conductivity relationship of polystyrene-block-poly(vinyl benzyl trimethylammonium) for alkaline anion exchange membrane fuel cells, *J. Polym. Sci. Polym. Phys.*, 51 (2013) 1751–1760.
- [27] Y.M. Zhang, J. Fang, Y.B. Wu, H.K. Xu, X.J. Chi, W. Li, Y.X. Yang, G. Yan, Y.Z. Zhuang, Novel fluoropolymer anion exchange membranes for alkaline direct methanol fuel cells, *J. Colloid Interface Sci.*, 381 (2012) 59–66.
- [28] C. Fujimoto, D.S. Kim, M. Hibbs, D. Wroblewski, Y.S. Kim, Backbone stability of quaternized polyaromatics for alkaline membrane fuel cells, *J. Membr. Sci.*, 423 (2012) 438–449.
- [29] X.H. Li, G.H. Nie, J.X. Tao, W.J. Wu, L.C. Wang, S.J. Liao, Assessing the influence of side-chain and main-chain aromatic benzyltrimethyl ammonium on anion exchange membranes, *ACS Appl. Mater. Interfaces*, 6 (2014) 7585–7595.
- [30] G.L. Han, P.Y. Xu, K. Zhou, Q.G. Zhang, A.M. Zhu, Q.L. Liu, Fluorene-containing poly(arylene ether sulfone) block copolymers: synthesis, characterization and application, *J. Membr. Sci.*, 464 (2014) 72–79.
- [31] X.H. Li, Y.F. Yu, Q.F. Liu, Y.Z. Meng, Synthesis and properties of anion conductive multiblock copolymers containing tetraphenyl methane moieties for fuel cell application, *J. Membr. Sci.*, 436 (2013) 202–212.
- [32] N.W. Li, Y.J. Leng, M.A. Hickner, C.Y. Wang, Highly stable, anion conductive, comb-shaped copolymers for alkaline fuel cells, *J. Am. Chem. Soc.*, 135 (2013) 10124–10133.
- [33] H.S. Dang, E.A. Weiber, P. Jannasch, Poly(phenylene oxide) functionalized with quaternary ammonium groups via flexible alkyl spacers for high-performance anion exchange membranes, *J. Mater. Chem. A*, 3 (2015) 5280–5284.
- [34] Z. Liu, X.B. Li, K.Z. Shen, P.J. Feng, Y.N. Zhang, X. Xu, W. Hu, Z.H. Jiang, B.J. Liu, M.D. Guiver, Naphthalene-based poly(arylene ether ketone) anion exchange membranes, *J. Mater. Chem. A*, 1 (2013) 6481–6488.
- [35] A. Jasti, S. Prakash, V.K. Shahi, Stable and hydroxide ion conductive membranes for fuel cell applications: chloromethylation and amination of poly(ether ether ketone), *J. Membr. Sci.*, 428 (2013) 470–479.
- [36] Z.J. Xia, S. Yuan, G.P. Jiang, X.X. Guo, J.H. Fang, L.L. Liu, J.L. Qiao, J. Yin, Polybenzimidazoles with pendant quaternary ammonium groups as potential anion exchange membranes for fuel cells, *J. Membr. Sci.*, 390 (2012) 152–159.
- [37] T. Sata, K. Kawamura, K. Matsusaki, Electrodialytic transport properties of anion-exchange membranes prepared from poly(vinyl alcohol), poly(N-ethyl 4-vinylpyridinium salt) and beta-cyclodextrin, *J. Membr. Sci.*, 181 (2001) 167–178.
- [38] O.I. Deavin, S. Murphy, A.L. Ong, S.D. Poynton, R. Zeng, H. Herman, J.R. Varcoe, Anion-exchange membranes for alkaline polymer electrolyte fuel cells: comparison of pendent benzyltrimethylammonium- and benzylmethylimidazolium-head-groups, *Energy Environ. Sci.*, 5 (2012) 8584–8597.
- [39] X.C. Lin, L. Wu, Y.B. Liu, A.L. Ong, S.D. Poynton, J.R. Varcoe, T.W. Xu, Alkali resistant and conductive guanidinium-based anion-exchange membranes for alkaline polymer electrolyte fuel cells, *J. Power Sources*, 217 (2012) 373–380.
- [40] J. Ran, L. Wu, J.R. Varcoe, A.L. Ong, S.D. Poynton, T.W. Xu, Development of imidazolium-type alkaline anion exchange membranes for fuel cell application, *J. Membr. Sci.*, 415 (2012) 242–249.
- [41] Y.P. Zha, M.L. Disabb-Miller, Z.D. Johnson, M.A. Hickner, G.N. Tew, Metal-cation-based anion exchange membranes, *J. Am. Chem. Soc.*, 134 (2012) 4493–4496.
- [42] K.J.T. Noonan, K.M. Hugar, H.A. Kostalik, E.B. Lobkovsky, H.D. Abruna, G.W. Coates, Phosphonium-functionalized polyethylene: a new class of base-stable alkaline anion exchange membranes, *J. Am. Chem. Soc.*, 134 (2012) 18161–18164.
- [43] A. Campione, L. Gurreri, M. Ciofalo, G. Micale, A. Tamburini, A. Cipollina, Electrodialysis for water desalination: a critical assessment of recent developments on process fundamentals, models and applications, *Desalination*, 434 (2018) 121–160.
- [44] X. Chen, Y.L. Jiang, S.S. Yang, J.F. Pan, R.J. Yan, B. Van der Bruggen, A. Sotto, C.J. Gao, J.N. Shen, Internal cross-linked anion exchange membranes with improved dimensional stability for electrodialysis, *J. Membr. Sci.*, 542 (2017) 280–288.
- [45] M. Manohar, A.K. Das, V.K. Shahi, Alternative preparative route for efficient and stable anion-exchange membrane for water desalination by electrodialysis, *Desalination*, 413 (2017) 101–108.
- [46] T. Chakrabarty, S. Prakash, V.K. Shahi, End group cross-linked 2-(dimethylamino) ethylmethacrylate based anion exchange membrane for electrodialysis, *J. Membr. Sci.*, 428 (2013) 86–94.
- [47] B.G. Shah, V.K. Shahi, S.K. Thampy, R. Rangarajan, P.K. Ghosh, Comparative studies on performance of interpolymer and heterogeneous ion-exchange membranes for water desalination by electrodialysis, *Desalination*, 172 (2005) 257–265.
- [48] S.X. Zhong, W.J. Wu, B.W. Wei, J. Feng, S.J. Liao, X.H. Li, Y.G. Yu, Influence of the ions distribution of anion-exchange membranes on electrodialysis, *Desalination*, 437 (2018) 34–44.
- [49] L. Chen, D. Wang, Z. Zhang, Study on the synthesis of 2,2',6,6'-tetramethylbiphenol, *Chem. Eng. Equip.*, 5 (2010) 15–17.
- [50] X.H. Li, L.C. Wang, S.S. Cheng, Investigation on structure and properties of anion exchange membranes based on tetramethylbiphenol moieties containing copoly(arylene ether)s,

- J. Appl. Polym. Sci., 132 (2015), <https://doi.org/10.1002/app.41525>.
- [51] X.H. Li, J.X. Tao, G.H. Nie, L.C. Wang, L.H. Li, S.J. Liao, Cross-linked multiblock copoly(arylene ether sulfone) ionomer/nano-ZrO₂ composite anion exchange membranes for alkaline fuel cells, *RSC Adv.*, 4 (2014) 41398–41410.
- [52] X. Yue, W.J. Wu, G.D. Chen, C.R. Yang, S.J. Liao, X.H. Li, Influence of 2,2',6,6'-tetramethyl biphenol-based anion-exchange membranes on the diffusion dialysis of hydrochloride acid, *J. Appl. Polym. Sci.*, 134 (2017), <https://doi.org/10.1002/app.45333>.
- [53] M.I. Khan, A.N. Mondal, B. Tong, C.X. Jiang, K. Emmanuel, Z.J. Yang, L. Wu, T.W. Xu, Development of BPPO-based anion exchange membranes for electro dialysis desalination applications, *Desalination*, 391 (2016) 61–68.
- [54] P.P. Sharma, V. Yadav, A. Rajput, V. Kulshrestha, PVDF-g-poly (styrene-co-vinylbenzyl chloride) based anion exchange membrane: High salt removal efficiency and stability, *Desalination*, 444 (2018) 35–43.
- [55] B.C. Lin, L.H. Qiu, B. Qiu, Y. Peng, F. Yan, A soluble and conductive polyfluorene ionomer with pendant imidazolium groups for alkaline fuel cell applications, *Macromolecules*, 44 (2011) 9642–9649.
- [56] M.I. Khan, R. Luque, S. Akhtar, A. Shaheen, A. Mehmood, S. Idress, S.A. Buzdar, A. Ur Rehman, Design of anion exchange membranes and electro dialysis studies for water desalination, *Materials*, 9 (2016) pii: E365, doi: 10.3390/ma9050365.